

Process of Diamond Surface Termination by Carboxylic and Amino Groups: A Quantum Mechanics Approach

Yuan Tian and Karin Larsson*

Department of Chemistry, Ångström Laboratory, Uppsala University, Uppsala, Sweden

Abstract

The main goal with the present work has been to study the possibility and thermodynamic stability for a sequential termination with either carboxylic groups (COOH), or amino groups (NH₂), from an initially H-terminated diamond (111) or 100)-2x1 surface. It was shown that it is energetically preferable to terminate both types of surfaces with up to 50% with COOH species. Moreover, it was shown possible to terminate both types of surface with up to 100% coverage with NH₂ species. In order to follow bond energy variations with variations in surface coverage, the averaged adsorption energies were also calculated. As expected, the lowest COOH coverage (of 6.25 %) resulted in the energetically most preferable adsorption energies. The situation with the NH₂ group was identical for the diamond (111) surface, with the lowest surface coverage (of 6.25%) leading to the most preferable adsorption situation. For the situation with diamond (100)-2x1, the preferable adsorption situation was for a surface coverage of 43.75% NH₂ species.

Partial Density of States (pDOS's) were also calculated with the purpose to analyse the adsorbate-induced surface electronic properties. COOH-terminated diamond (100)-2x1 surface, as well as COOH- and NH₂-terminated diamond (111) surfaces, were shown to display surface conductivities which were not observed for 100% H-terminated surfaces.

Keywords: Diamond; Theory; DFT-calculations; Surface termination; Surface modification; COOH; NH₂

Introduction

Since first successful synthesis of diamond, it has attracted extensive research interests. That is mainly due to its unique properties, e.g., hardness, chemical inertness [1], large electrochemical potential window [2], biocompatibility [3,4], and desirable optical properties [5]. As the result of intense development of diamond synthesis techniques, nanocrystalline diamond films and nanodiamond particles have aroused a large interest interests within various research fields [6]. Moreover, it has also been reported that the surface properties of diamond can easily be modified by using various approaches, which have provided a versatile platform for different applications. The surface modification techniques can be mainly grouped as: (1) terminations of the diamond surfaces [7], and (2) substitution doping of the diamond lattice (N [8], B [9], and others [10]). For example, diamond surfaces terminated with hydrogen has been found to be hydrophobic and to have a surface electronic conductivity [2,11]. The oxygen-terminated diamond surfaces are though hydrophilic and insulating [12]. Substitution doping of diamond has also been found to dramatically change the materials properties. Non-doped diamond is an insulator, while B-, or N-doping, will give semiconducting properties [13]. These findings enlighten the possibility of manipulating both the bulk and surface conductivity, which makes diamond a promising material for different applications (e.g., biosensing [14]). The possibilities for surface termination and functionalization, in addition to the fact that diamond is biocompatible and chemically inert, make diamond a good substrate for various biological applications (e.g., drug delivery [15], diagnostic tools [16], immunoassays [17], and biomedical applications [18,19]).

In order to immobilize proteins on a diamond surface at a higher dosage and with improved stability, a large number of research efforts have been conducted in the last years. It is reported, and widely recognized, that the hydrophilicity usually facilitates the immobilization of protein and biomolecules onto diamond surfaces [20,21]. Surface charges associated with functional groups are also believed to be a

determining factor for protein adsorption [22]. When comparing the different surface terminations groups, each of them displays pros and cons for different protein functionalization [7]. Oxygen-related terminations, which include carbonyl (C=O), peroxide-type (O-O), carboxylic acid (COOH), cyclic ether (COC), and carboxylic anhydride (C=O-O-C=O), are beneficial for protein immobilization mainly for their good surface wettability. In addition, due to the resemblance of the COOH group with protein residues, the COOH adsorbates may react with the NH₂ species on the protein surfaces, forming amine bonds that will further improve the protein adsorption strengths. Therefore, the COOH species is a promising surface termination candidate, as compared with the other oxygen-containing groups [23]. Theoretical studies of oxygenated diamond surfaces (including O-ontop and O-bridge termination) have been conducted by several groups [24,25], and they have been found to provide a sound foundation for experiments. However, more detailed theoretical studies of COOH-terminated diamond surfaces, and information about how COOH will affect the surface properties, are still missing.

Similar to COOH-termination, the NH₂ adsorbates resemble the protein residues and are thereby expected to be able to react with carboxylic groups and to form amine bonds with the biomolecules surfaces. This terminating species is beneficial for the biomolecule adsorption strength, and for further surface functionalization [26]. Diamond surface termination with amino groups are usually achieved

*Corresponding author: Karin Larsson, Department of Chemistry, Ångström Laboratory, Uppsala University, Uppsala, Sweden, Tel: +46 70 3903750; E-mail: karin.larsson@kemi.uu.se

Received January 07, 2019; Accepted January 10, 2019; Published January 20, 2019

Citation: Tian Y, Larsson K (2019) Process of Diamond Surface Termination by Carboxylic and Amino Groups: A Quantum Mechanics Approach. J Material Sci Eng 8: 506. doi: 10.4172/2169-0022.1000506

Copyright: © 2018 Tian Y, et al. This is an open-access article distributed under the terms of the Creative Commons Attribution License, which permits unrestricted use, distribution, and reproduction in any medium, provided the original author and source are credited.

by (i) UV-irradiation of diamond in ammonia gas environment [27,28], (ii) electrochemical attachment in basic solution, and (iii) photochemical attachment with protection groups [26]. The experimental surface coverage is estimated to be around 10% [29]. Facet-dependent adsorption behaviours has earlier been shown in a theoretical study, using Density Functional Tight Binding techniques and the following terminating species; N, NH, and NH₂. The diamond (100) facet was thermodynamically preferred for all of these terminating species. However, a theoretical study of the NH₂-termination onto diamond surfaces, as a function of coverage, is not yet fully understood.

In order to gain a better understanding of the effect by COOH and NH₂ termination on (i) the diamond surface properties, and (ii) on the possibility to use in the immobilisation of biomolecules, calculations have in the present performed by using Density Functional Theory (DFT) techniques under boundary periodic conditions. Diamond (111) and (100)-2x1 surfaces were chosen due to their abundants on synthetic diamond [30-34]. These surface planes were initially completely terminated by H. These H adsorbed where thereafter sequentially replaced with either COOH (or NH₂) groups at the following surface coverages: 0%, 6.25%, 12.5%, 18.75%, 25%, 31.25%, 37.5%, 43.75%, 50%, 56.25%, 62.5%, 68.75%, 75%, 81.25%, 87.5%, 93.75% and 100%. Energetic, geometrical, and electronic conductivity properties of the diamond surfaces, as a function of surface termination coverage, where especially focused in the present study.

Methods, Methodologies and Models

In order to study the geometrical structures and electron distributions for the different diamond surface systems, a density functional theory (DFT) method was used. It was based on an ultrasoft pseudopotential [35] plane-wave approach, and available within the Cambridge Sequential Total Energy Package (CASTEP) program from Accelrys, Inc [35]. By using the spin-polarized Generalized Gradient Approximation (GG(S)A-PW91), developed by Wu and Cohen [31], the electronic exchange and correlation corrections were approximated [36,37]. In contradiction to the simplest Local Density Approximation (LDA), the GGA method describes the density inhomogeneity within the system by using an electron density gradient expansion [31]. The GGA methods are generally known to be more accurate than the Local Density Approximations (LDA). The LDA method is known to underestimate bond lengths and to over-bind electrons in a molecule [32]. Within the present study, the energy cut-off for the plane-wave kinetic was set to 300.00 eV. The k-point mesh (generated from the Monkhorst-Pack scheme [33]) used for all calculations was set to 1x1x1, which were proven to be sufficient for similar system [34].

Because of the expected strong correlation between bond energy and electron bond populations/atomic charges for polar covalent bonds, further analyses of electron bond populations and degree of electron transfer within the bonds have been made in the present study. To estimate the atomic charges, a portioning of the Mulliken charge to individual atoms where made by projecting the plane wave states onto the localized basis set [38,39]. The electron bond population is an estimation of the density of electrons within the bonds and is thereby also regarded as a measure of the covalent bond strength. A more general covalent bond most often shows a certain degree of polarity (i.e., ionicity). Hence, calculations of atomic charges will give a measure of the ionic contribution to the bond strength.

In order to simulate the process of surface termination with COOH (or NH₂) groups, starting from a completely H-covered diamond (111) or diamond (100)-2x1 surface, each surface H adsorbate has

been sequentially replaced by one COOH (or NH₂) species (i.e., from a COOH (or NH₂) surface coverage of 0% towards 100%). For each specific coverage, the individual COOH species were positioned on the surface in a way to minimize the inter COOH (or NH₂) electrostatic repulsions. For each of these situations, both total (eq. 1) and average adsorption energies (eq. 2) have been calculated;

$$E_{ads} = E_{Dia-nR} - E_{Dia-(16-n)H} - n E_{*R} \quad (1)$$

$$E_{ads, avr} = 1/n (E_{Dia-nR} - E_{Dia-(16-n)H} - n E_{*R}) \quad (2)$$

$$E_{stab} = E_{ads} - E_H \quad (3)$$

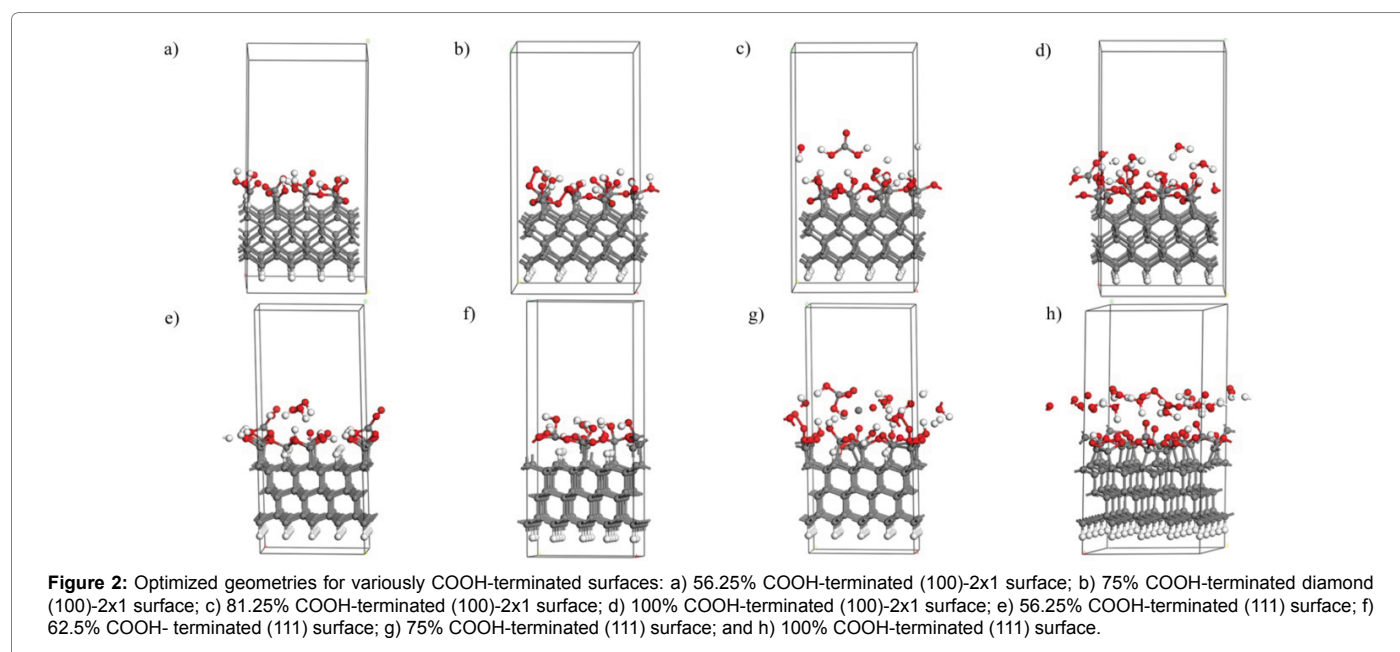
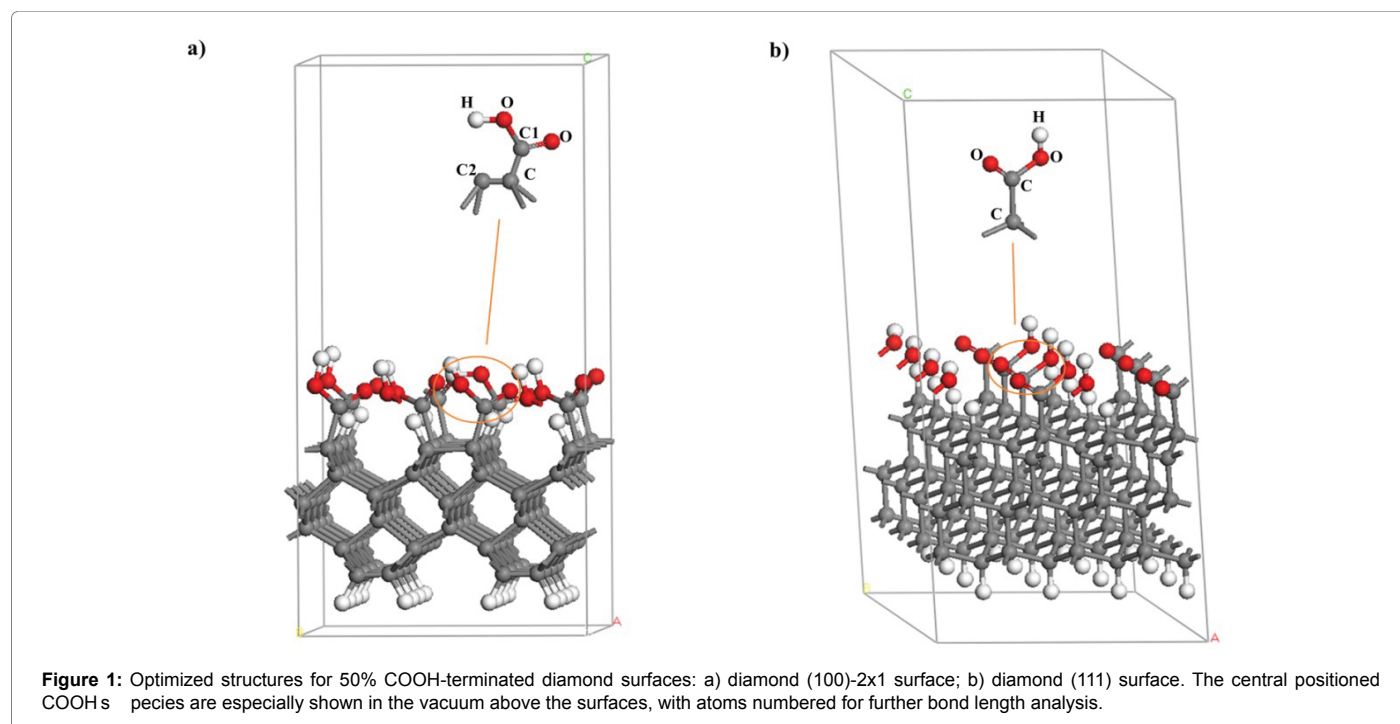
Where E_{Dia-nR} represent the total energy for the completely terminated diamond surface (with both H and COOH), and where $E_{Dia-(16-n)}$ represent the total energy for a surface that has a terminating layer that includes only H and non-terminated C radical sites. Moreover, E_{*R} represents the total energy for a molecular COOH species, where R denotes COOH and NH₂, respectively. Hence, the total adsorption energies indicate the energy for adsorption of n COOH (or NH₂) to a diamond surface that is covered with a mix of H adsorbates and non-terminated surface C radicals. Moreover, the average adsorption energy is simply the average in adsorption energy for these n COOH (or NH₂) adsorbates. E_{stab} denotes the relative stabilization energy, with respect to 100% H-termination. E_H is thereby the adsorption energy for a completely covered surface with H species. All of these total energies have been obtained from the geometry optimization of the model structures.

Due to their abundance in synthetic diamond materials, the following surface planes were used in modelling the various adsorption situations; diamond (111) and 2x1 reconstructed diamond (100) [35]. The surface models were constructed as super-cells, under periodic boundary conditions. These models consisted of six carbon layers, with 16 atoms in each of them with a 4x4 pattern (i.e., with a total of 96 C atoms). The models are visualized in Figures 1 and 3 for COOH and NH₂ terminations, respectively. Since the central H adsorbate is the first one to be substituted with the adsorbate COOH (or NH₂), this specific species (i.e., COOH or NH₂) will be used in the analysis of bond length as a function of surface coverage. In order to visualize these central located species on the surfaces, they are shown in the upper part of Figures 1 and 3). To avoid possible inter slab interactions, the lattice z parameter (i.e., the so called vacuum space) was set to 10 Å. In addition, the bottom dangling bonds were saturated with H atoms. The dangling bond-passivating H atoms, in addition to the two bottom layers, were held fixed during the calculations in order to simulate a continuous bulk structure. The rest of the atoms in the slab were allowed to fully relax during the geometry optimization calculations using the Broyden-Fletcher-Goldfarb-Shannon (BFGS) algorithm [36]. The viability of all of these theoretical and model-relating parameters has earlier been carefully evaluated for almost identical systems [28]. They are therefore assumed to be optimal to use for the purpose with the present investigation.

Results

Geometry structures

As presented in the Introduction, COOH- and NH₂-terminations display unique advantages as compared with, e.g., oxygen-related terminations. The reason is the possibility for them to form amine bonds with biomolecules terminus (Proteins, DNA, etc.) [7]. In order to provide further understanding of the two termination processes, the



adsorption of carboxylic acid (COOH) and amino (NH_2) groups to diamond (100)-2x1 and (111) surfaces, have in the present work been theoretically investigated.

In comparison to smaller termination species (e.g., H, and OH), it was in the present study not found possible to completely cover a surface with COOH species. In fact, it was only found possible to terminate the diamond (100)-2x1 and (111) surfaces up to 50 % with COOH species, with the rest of the surface carbons terminated with H species (Figure 2). When initially terminating the surfaces with a higher COOH coverage, some of the adsorbates were found to desorb from the

surface; either in the form of molecular COOH, or as COOH-related fragments (some of them are displayed in Figure 2).

For a 2x1-reconstructed diamond (100) surface, a cross-linking between surface C and O (within COOH) were observed to take place for surface coverages between 56.25% (Figure 2a) and 75% (Figure 2b). With start from 81.25 % (Figure 2c) and up to 100% (Figure 2d), desorption of COOH-related species was observed to take place. For a diamond (111) surface, desorption of COOH-related species from the surface was observed to take place at a lower surface coverage; from 56.25% until 100% (Figures 2e-2h). In addition, cross linking between

surface C atoms and the COOH species was found to result in O_{bridge} positions (Figure 2a). Another type of surface modification at these higher surface COOH coverages was the O-O bond formation between neighbouring COOH adsorbates (Figure 2b).

For both types of diamond surface planes, the COOH-related fragments, that were desorbed from the surface, involved water molecules (Figure 2c) and H_2CO_3 (Figure 2g). The fact that fragments start to desorb from the diamond (111) surface at a lower COOH coverage is most probably due to the difference in surface C concentration between diamond (100)-2x1 and diamond (111); 0.18 atom/ \AA^2 vs. 0.16 atom/ \AA^2 . The higher surface C concentration ultimately causes higher degree of crowdedness amongst the COOH adsorbates.

Compared to COOH, NH_2 is a smaller molecule and are not predicted to undergo bond breakages or reconstructions when covering the diamond surfaces. In fact, there were no sign of surface reconstruction for any coverage concentration. In Figure 3, structures of 100% terminated diamond (100)-2x1 surface (Figure 3a), and diamond (111) surface (Figure 3b) are displayed.

Bond lengths within central terminated groups

In order to further determine the structural influences by the surface terminating species, bond lengths for central terminating species were compared as a function of termination coverage (Figures 1 and 3 for an identification of these groups). The C-C, C-O, and C=O bond lengths for COOH are shown in Tables 1 and 2, while the C-C, C-N and N-H within NH_2 are shown in Tables 3 and 4.

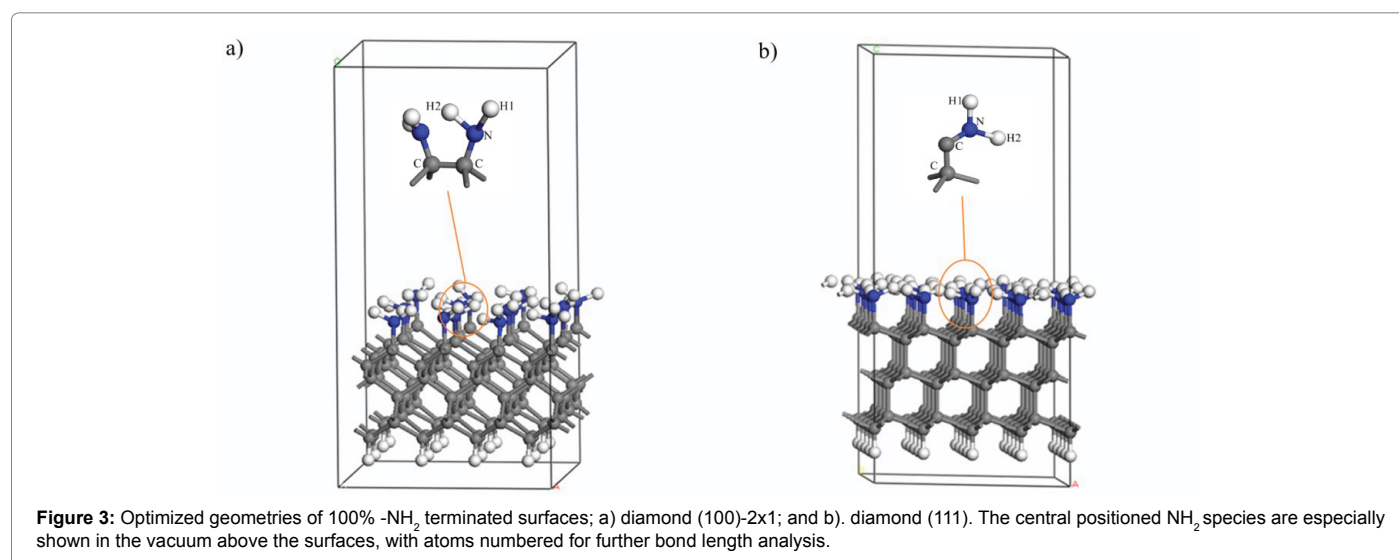
As presented in *Geometry structures* above, it is not possible to COOH-terminate a diamond (111) or (100)-2x1 surface to more than 50%. At higher surface coverages, fragments of the adsorbates will be desorbed from the surfaces. As can be seen in Tables 1 and 2, the various COOH bond lengths were observed to increase at a higher surface coverage. The experimental bond lengths are the following; 1.5-1.7 (C-C), 1.1-1.3 (C=O), 1.3-2.1 (C-O), and 0.9-1.2 (OH) \AA [37,38]. For a surface coverage increase from 0 to 62.5% for diamond (100)-2x1 surface, the COOH bond lengths were observed to reside in the experimental bond lengths regions. For the diamond (111) surface, this was the situation for a surface coverage increase from a 0 to 50% surface COOH coverage. However, when the coverages increased above these

upper limits some bond lengths became unrealistic long, most probably representing bond breakages (marked in red). When comparing these values with the bond lengths obtained here, some bond lengths, e.g. 5.21 \AA for C=O, 4.21 \AA for O-H, or 2.76 \AA for C-O, are not realistic for bonding situations. The causes to these bond length elongations are most probably the severe sterical hindrances amongst the COOH adsorbates.

The situation for NH_2 termination is easier to analyse. The experimental bond lengths of C-C, C-N and N-H are 1.5-1.6 \AA , 1.4-2.1 \AA and 1.0-1.4 \AA [38]. When comparing the experimental values with bond lengths above, all values are situated within the experimental ranges of bond lengths. Therefore, NH_2 termination does not endure sterical hindrances and forms stabilized structures for coverage up to 100%.

Concentration (%)	Diamond (100)-2x1 Bond Length (\AA)				
	C-C1	C-C2	C=O	C-O	O-H
6.25%	1.53	1.60	1.22	1.37	0.98
12.5%	1.53	1.60	1.22	1.37	0.980
18.75%	1.52	1.61	1.22	1.40	0.98
25%	1.53	1.59	1.22	1.37	0.98
31.25%	1.52	1.61	1.24	1.33	0.99
37.5%	1.50	1.61	1.23	1.34	0.99
43.75%	1.51	1.59	1.25	1.32	0.99
50%	1.50	1.59	1.22	1.35	0.98
56.25%	1.58	1.58	1.30	1.49	1.00
62.5%	1.53	1.56	1.27	1.35	0.98
68.75%	1.60	1.55	1.43*	1.40	0.98
75%	1.50	1.52	1.36*	1.52	2.05*
81.25%	1.51	1.54	1.42*	1.35	1.94*
87.5%	1.52	1.56	3.16*	1.39	1.67*
93.75%	1.72*	1.53	1.46*	1.40	5.55*
100%	1.92*	1.55	1.42*	2.76*	1.00

Table 1: C-C, C=O, C-O, and O-H bond lengths (within the central COOH adsorbate as shown Figure 1), as a function of COOH diamond (100)-2x1 surface coverage. The "bond lengths" which exceed experimental values are marked with an asterisk. Surface coverages for which cross linking between the adsorbate and the surface takes place, are marked in yellow. Surface coverages for which desorption of fragments takes place, are marked in red.



Adsorption energies and average adsorption energies

As presented in the *Introduction*, terminating species on the diamond surfaces have been found to have a strong influence on the chemical properties of these surfaces (e.g., surface electrostatic properties, water solubility and lipophilicity) [39]. In the determination of energetic preferences for optimal surface coverage, adsorption energies of the surface termination groups (COOH and NH₂) have been calculated and compared with 100% H-terminated (Figures 4 and 6). These relative stabilization energies visualised as a function of coverage in Figures 4 and 6 for both diamond (100)-2x1 and diamond (111) surfaces. For the situation with COOH-termination, various types of fragments start to desorb from the surface for a surface COOH coverage above 56%. The onset of surface reconstruction and desorption from the surface, are especially marked in Figure 4. For the (100)-2x1 surface, the adsorption energies reach a minimum (-26.2 eV) at a COOH surface coverage of 50% (Figure 4a). The adsorption energy per

Concentration (%)	Diamond (111) Bond Length (Å)			
	C-C	C=O	C-O	O-H
6.25%	1.56	1.23	1.38	0.99
12.5%	1.56	1.23	1.37	0.99
18.75%	1.56	1.23	1.36	0.99
25%	1.57	1.23	1.37	0.98
31.25%	1.56	1.22	1.37	0.98
37.5%	1.57	1.24	1.33	0.98
43.75%	1.60	1.23	1.35	0.98
50%	1.60	1.23	1.35	0.98
56.25%	1.60	1.33*	1.53	2.62*
62.5%	1.53	1.38*	1.40	2.05*
68.75%	1.49	2.08*	1.24	1.71*
75%	1.52	1.49*	1.42	1.98*
81.25%	1.51	3.50*	1.34	2.97*
87.5%	1.53	4.19*	1.38	3.40*
93.75%	1.60	5.21*	1.33	4.21*
100%	1.57	4.85*	2.50*	1.02

Table 2: C-C, C=O, C-O, and O-H bond lengths (within the central COOH adsorbate as shown in Figure 1) as a function of COOH diamond (111) surface coverage. The "bond lengths" which exceed experimental values are marked with an asterisk. The surface coverages for which desorption of fragments takes place, are marked in red.

Concentration (%)	Diamond (100)-2x1 Bond Length (Å)				
	C-C	C-N	N-H1	N-H2	N-H Mean
6.25%	1.60	1.47	1.02	1.02	1.02
12.5%	1.60	1.47	1.02	1.02	1.02
18.75%	1.60	1.47	1.02	1.02	1.02
25%	1.60	1.47	1.02	1.02	1.02
31.25%	1.60	1.47	1.03	1.02	1.03
37.5%	1.60	1.47	1.03	1.02	1.03
43.75%	1.60	1.47	1.03	1.02	1.03
50%	1.60	1.47	1.02	1.02	1.02
56.25%	1.61	1.47	1.03	1.02	1.03
62.5%	1.60	1.47	1.03	1.02	1.03
68.75%	1.60	1.47	1.02	1.02	1.02
75%	1.59	1.48	1.02	1.02	1.02
81.25%	1.59	1.48	1.03	1.02	1.03
87.5%	1.57	1.49	1.04	1.02	1.03
93.75%	1.65	1.48	1.03	1.03	1.03
100%	1.60	1.47	1.02	1.02	1.02

Table 3: C-C, C-N, N-H1, and N-H2 bond lengths (within the central NH₂ adsorbate as shown in Figure 3) of as a function of NH₂ diamond (100)-2x1 surface coverage.

Concentration (%)	Diamond (111) Bond Length (Å)			
	C-N	N-H1	N-H2	N-H Mean
6.25%	1.48	1.02	1.02	1.02
12.5%	1.49	1.02	1.02	1.02
18.75%	1.49	1.02	1.02	1.02
25%	1.48	1.02	1.02	1.02
31.25%	1.49	1.02	1.02	1.02
37.5%	1.49	1.02	1.02	1.02
43.75%	1.49	1.02	1.02	1.02
50%	1.50	1.02	1.03	1.03
56.25%	1.50	1.03	1.03	1.03
62.5%	1.51	1.02	1.03	1.03
68.75%	1.50	1.02	1.05	1.04
75%	1.50	1.02	1.02	1.02
81.25%	1.49	1.04	1.02	1.03
87.5%	1.48	1.08	1.05	1.07
93.75%	1.48	1.03	1.01	1.02
100%	1.47	1.00	1.22	1.11

Table 4: C-N, N-H1, N-H2, mean value of N-H Bond lengths (within the central NH₂ adsorbate as shown in Figure 3) as a function of NH₂ diamond (111) surface coverage.

COOH (i.e., the averaged adsorption energy) species varies between -5.5 and -2.0 eV when increasing the COOH surface coverage from zero to 50%. The adsorption energy for the lowest surface coverage (6%) in the present study (i.e., corresponding to the situation when only one surface C (in the super cell) was terminated with a COOH species) was the most profound one in the present study (-5.5 eV). This result indicates the preference for initial COOH-termination to these surfaces, especially in the lack of sterical hindrances from neighbouring COOH species.

The COOH adsorption energies for the diamond (111) surface are presented in Figure 4b. As was the situation with diamond (100)-2x1, the minimum adsorption energy (corresponding to the strongest adsorption) was obtained at a COOH surface coverage of ~50%, with a value of -17.8 eV. As presented above, when the COOH coverage exceeded 50%, the adsorbate structure reconstructed at a specific surface coverage of 75% and 87.5%, respectively (with a corresponding decrease in total adsorption energy).

The results for both of the diamond (111) and (100)-2x1 surfaces show that the substitutional termination with COOH (instead of H) will be energetically preferred up to a surface coverage of about 50%. In addition, it was also found that the COOH adsorption (at about a surface coverage of 50%) onto the diamond (100)-2x1 surface (-26.2 eV) was stronger as compared with the diamond (111) surface (-17.8 eV). The underlying reason for this energetic preference can also be supported by higher surface C density for diamond (111) surface (0.18 C atom/Å²) compared with diamond (100)-2x1 (0.16 C atom/Å²), which results in higher sterical hindrances for the diamond (111) surface plane.

These observations are in good agreement with experimental results by Wang, et al. [40]. They showed that the surface coverage by carboxylic acid (by a wet chemistry approach) is 9.2% (diamond (100)-2x1) and 4.7% (diamond (111)).

Averaged values adsorption energies are useful tools in following the adsorption process step-by-step. Those values give information about how difficult it might be for specific terminators to bind to a surface. The averaged adsorption energies for a COOH adsorbate binding to diamond (100)-2x1, and (111), respectively, are displayed as

a function of surface termination coverage in Figure 5. With an increase in coverage, average adsorption energies were observed to increase from -5.45 to -3.28 eV for diamond (100)-2x1, and from -5.10 to -2.23 eV for diamond (111) surface. These results give a picture over the difficulties for COOH species to bind to the surfaces when the surface coverage increases.

In Figure 6, total adsorption energies for NH₂-termination onto

diamond (100)-2x1 and diamond (111) surfaces, are mapped as a function of surface coverage. For the diamond (100)-2x1 surface (Figure 6a), the adsorption energies were found to drop from initially -3.83 eV for the first NH₂ termination to -45.84 eV for 100% coverage. The average adsorption energy (i.e., for an individual NH₂ adsorbate), was observed to change from -3.98 to -1.08 eV and the graph is quite linear as compared with COOH termination. This result suggests a

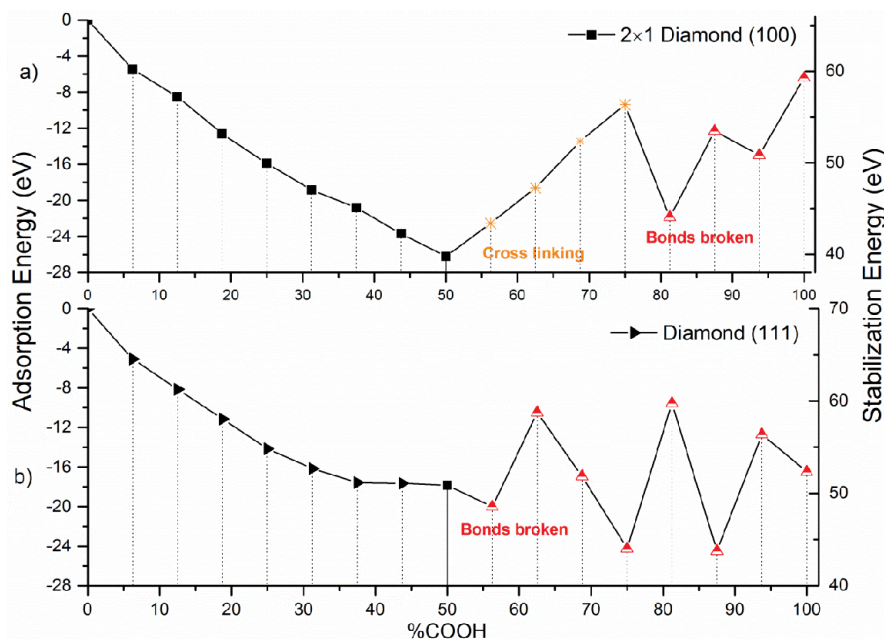


Figure 4: Adsorption (left Y axis) and stabilization energies (right Y axis) of COOH-termination species as a function of increasing COOH surface coverage on an otherwise H-terminated diamond surface. Modified surface structures are marked with yellow (cross linking) and red (bonds broken); a) diamond (100)-2x1, b) and diamond (111).

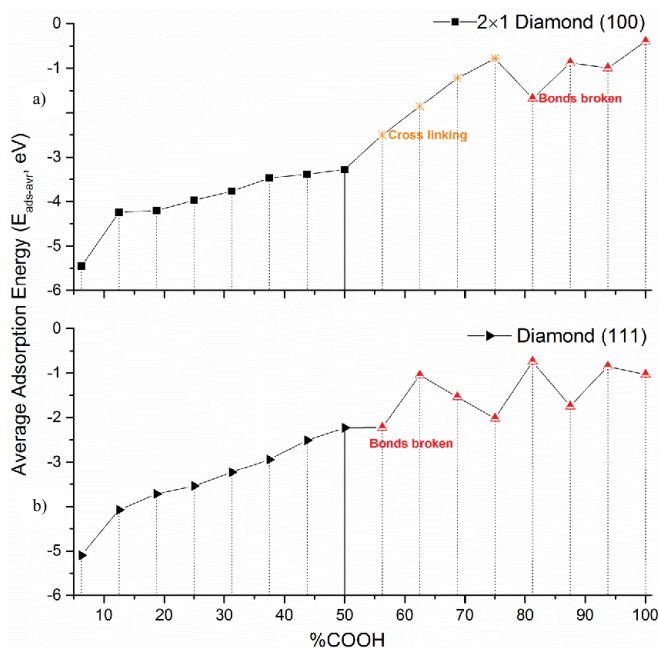


Figure 5: Average adsorption energies of surface termination species (-COOH) as a function of increasing COOH-coverage on an otherwise H-terminated diamond surface. Modified surface structures are marked with yellow (cross linking) and red (bonds broken); a) diamond (100)-2x1, b) and diamond (111).

successive energetically stability of NH_2 terminations on the diamond (100)-2 \times 1 surface (Appendix 1).

A similar situation was observed for diamond (111) surface (Figure 6b), for which the total adsorption energies were found to decrease from -3.61 eV (6.25%) to a minimum of -39.91 eV (100%). The corresponding average adsorption energies were found to ranges from -3.61 to -1.49 eV. These results suggest that fully -NH_2 terminated surfaces are the most energetically stable surfaces for both surface planes. When comparing the results for the two surface planes, the total adsorption energies for surface NH_2 groups onto diamond (111) were calculated to be higher than those for diamond (100)-2 \times 1, which indicates that diamond (100) surface is energetically easier to functionalize with NH_2 groups. Moreover, the relative stabilization energies for both surface planes are positive from 0% to 100% coverage, which indicates that NH_2 termination is also less energetically preferred than H-termination.

In order to investigate the energetically preferences of successive steps for NH_2 termination, the average adsorption energies of surface NH_2 groups are, as a function of coverage, shown in Figure 7. For the diamond (100)-2 \times 1 surface, the average adsorption energies were observed to decrease from -3.83 (6.25%) to -3.95 eV (43.75%). This result shows the tendency for a thermodynamically seen easier termination step by the NH_2 species when the coverage increases from 0% until 43.75%. For the diamond (111) surface, it is somewhat more difficult to reach higher surface coverages as the average adsorption energies were observed to increase from -3.61 to -2.49 eV.

Surface partial density of states (pDOS)

In order to determine the influences on electronic properties by the studied surface terminations, the energetically most stabilized

structures for both surface terminations (50% COOH and 100% NH_2) were considered for further analysis. Partial Density of States (pDOS) were calculated in order to outline possible effects on the electronic structure (and, hence, on the surface electronic conductivity). Obtained results for diamond (100)-2 \times 1 are displayed in Figure 8, and the results for diamond (111) are shown in Figure 9. All results are compared with corresponding pDOS spectra for H-termination.

For a 100% H-terminated diamond (100)-2 \times 1 surface, a HOMO-LUMO gap of 2.6 eV was obtained (Figure 8a). When 50% surface H atoms were substituted with COOH groups, the HOMO-LUMO gap was still maintained at approximately 2.6 eV (Figure 8b). However, there was a partially filled site within the HOMO-LUMO gap that originated from surface COOH groups (Figure 8c). It must though be stressed that the magnitude of this peak is very minor. Another observation was made for the situation with a 100% NH_2 -terminated diamond (100)-2 \times 1 surface (Figure 8d). The HOMO-LUMO gap was then observed to decrease to 1.6 eV. For this situation, however, no distinct peak was observed within the HOMO-LUMO gap (Figures 8d and 8e). Based on these obtained results, it can be concluded that the semi-conductor properties will differ appreciably depending on type of surface termination.

For the situation with a 100% H-terminated diamond (111) surface, a HOMO-LUMO gap of 2.5 eV was observed (Figure 9a). For a surface coverage of 50% with COOH species, there was an observed shift in LUMO level to lower energy levels (Figure 9c). As compared with 100% H-termination, the HOMO-LUMO gap decreased to 1.5 eV (Figure 9b). However, in comparison to the diamond (100)-2 \times 1 surface, no peak within the HOMO-LUMO gap was observed. Moreover, for a 100% NH_2 -terminated diamond (111) surface (Figure 9d), the HOMO-

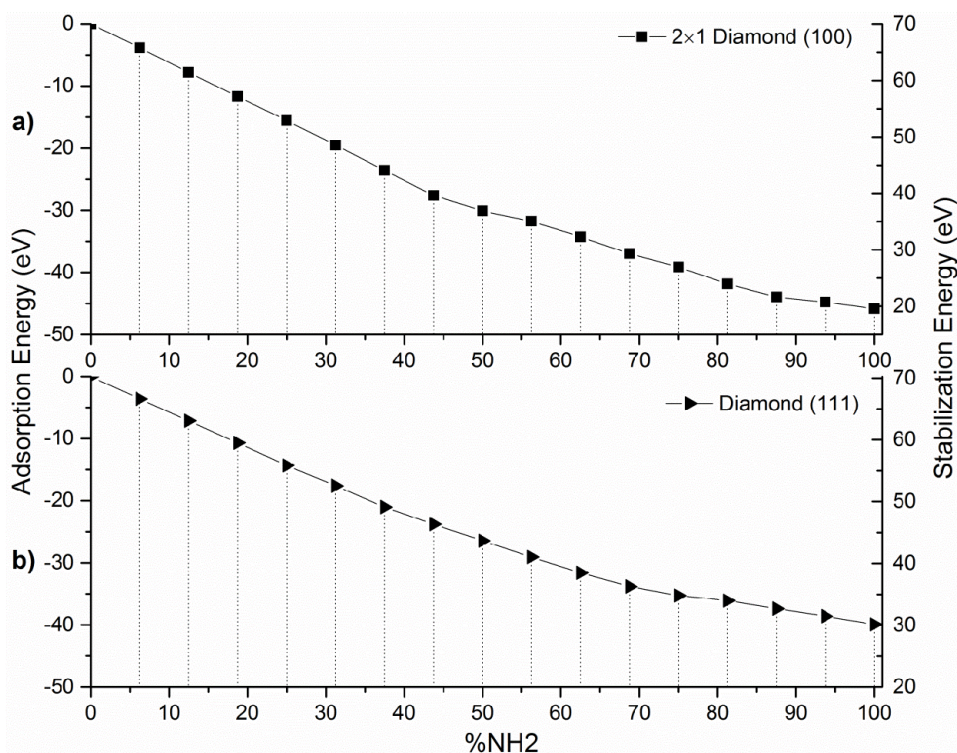
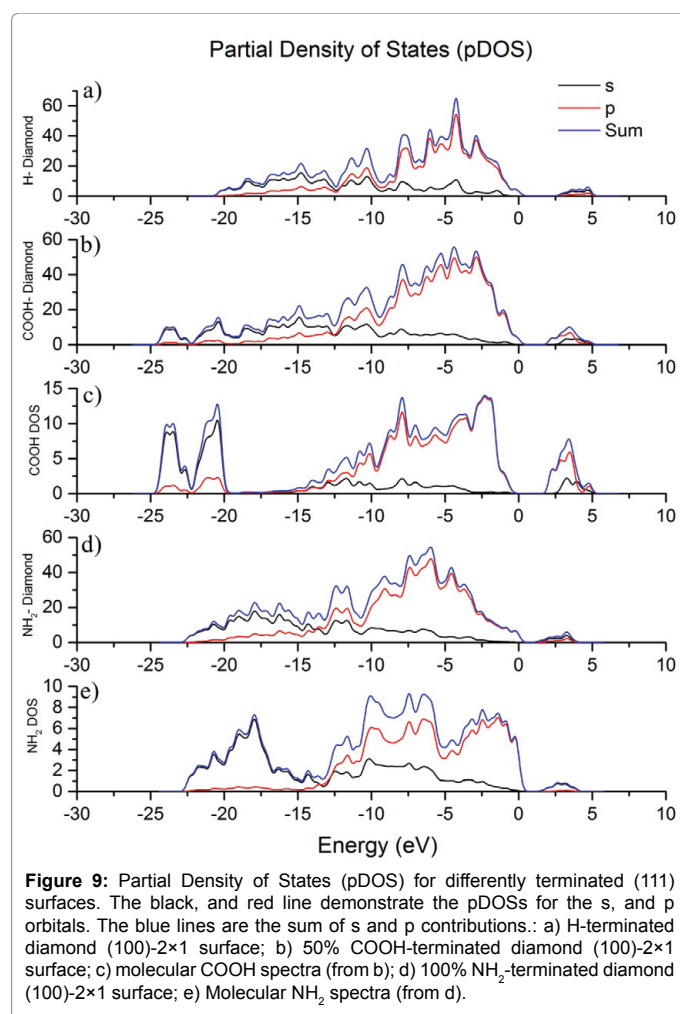
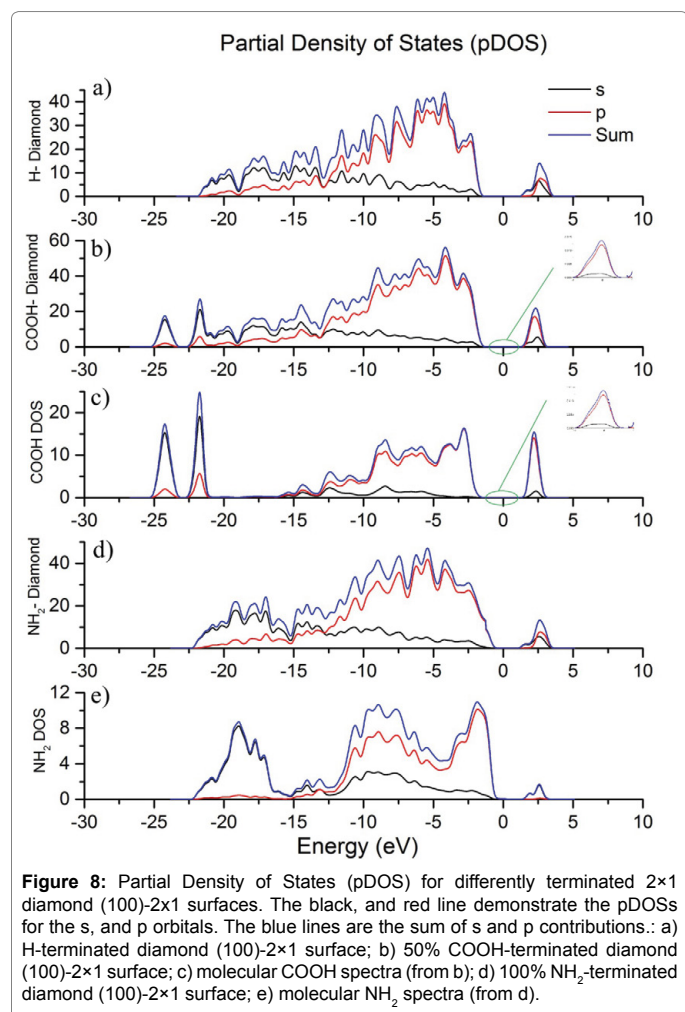
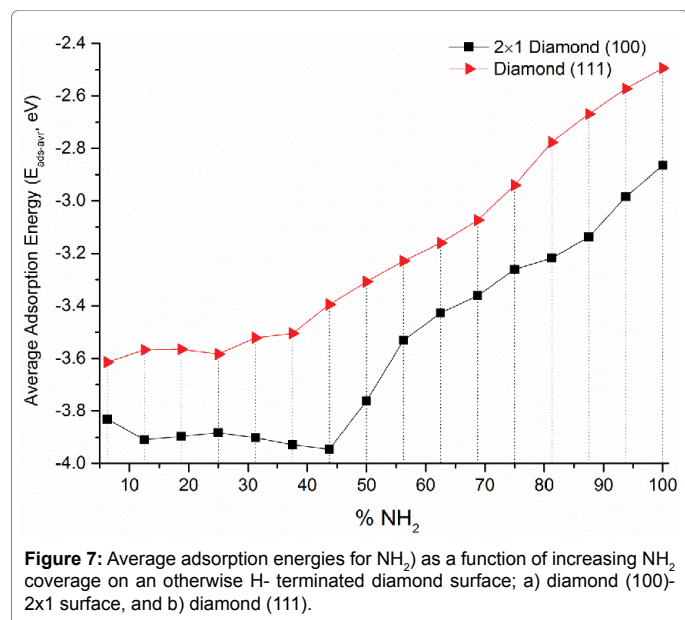


Figure 6: Adsorption (left Y axis) and stabilization energies (right Y axis) of NH_2 as a function of increasing NH_2 surface coverage on an otherwise H-terminated diamond surface; a) diamond (100)-2 \times 1 surface, and b) diamond (111).

LUMO gap was observed to decrease even further (down to 0.8 eV) (Figure 9d and 9e). First of all, it is possible to draw the conclusion that



the semi-conductor properties depend on type of diamond surface (i.e., diamond (111) will render a narrower HOMO-LUMO gap with COOH or NH_2 termination). Secondly, for the more sensitive diamond (111), 50% coverage with COOH will have a profound effect on the HOMO-LUMO gap (as compared with diamond (100)-2x1).

Summary and Conclusions

In the present theoretical study, the diamond surface coverage by COOH (or NH_2) species has been carefully examined (using DFT techniques) in search for the most energetically stable coverage degree. In addition, these most stable surface constellations were further analysed in order to gain information about their properties in form of surface electronic conductivity. These types of terminated surfaces have not earlier been studied in sufficient detail, and the main purpose was here to look for surface termination situations that both are stable and can be of use for applications where surface electron conductivity are of highest importance (e.g., renewable energy).

Total adsorption energies, averaged adsorption energies and relative stabilisation energies, where calculated for model systems where initially 100% H-terminated diamond surfaces were used. Thereafter, surface H species were step-wise replaced by COOH (or NH_2) in order to follow the evaluation of the two types of adsorption energies, as well as of the relative stabilisation energies, when going from a 0% COOH (or NH_2) termination towards 100%.

It can be concluded that for COOH-termination, a 50% coverage is the most energetically preferable surface concentration, for both diamond (100)-2x1 and diamond (111) surfaces. On the contrary, it has been shown possible to completely terminate both types of surfaces with NH₂ species. Moreover, the adsorption energies for these two surface terminating species show that it is easier to bind to the diamond (100)-2x1, which most probably depend on the quite large sterical hindrances amongst the adsorbates in combination with the somewhat lower surface C concentration of diamond (100)-2x1. Due to increasing, adsorbate-adsorbate interactions with surface coverage, it has here been proven more and more difficult to cover the diamond (100)-2x1 and diamond (111) surfaces with COOH groups. The same observation, but to a less extent, was made for the NH₂-terminated diamond (111) surface. Unexpectedly, this trend in energies was not observed for the NH₂-terminated diamond (100)-2x1 surface, for which the average adsorption energies decreased until a surface coverage of 43.75%. A plausible explanation to this observation is two-fold. At first, neighbouring NH₂ adsorbates will have the tendency to interact with each other by forming hydrogen bonds, and thereby stabilizing the surface. But, there is also the tendency for sterical repulsions at higher surface coverages. Secondly, the diamond (100)-2x1 surface has a smaller surface C concentration, which can explain why the sterical repulsions seem to start to dominate at a higher NH₂ surface coverage.

It was also observed that COOH- and NH₂-termination, respectively, will reduce the diamond surface HOMO-LUMO band gap. The effect was larger for diamond (111), compared to diamond. In fact, both COOH- and NH₂-termination caused a narrowing of the HOMO-LUMO gap, with dominance by NH₂. Similarly, only NH₂ was efficient in reducing the HOMO-LUMO gap for NH₂-terminated diamond (100)-2x1. Hence, the possibility for modification of surface electronic states, by simply terminating with these types of species, was the outcome of the present study.

Acknowledgement

This study was conducted with programs developed by Accelrys, Inc., and financially supported by the European Union Frame programme Seven (FP7) project, Vascubone, under grant number of 242175.

References

- Jackson M, Ahmed W (2007) Surface Engineered Surgical Tools and Medical Devices. Springer: New York.
- Hauf MV, Simon P, Seifert M, Holleitner AW, Stutzmann M, et al. (2014) Low Dimensionality of the Surface Conductivity of Diamond. *Phys Rev B* 89: 115426-115435.
- Tang L, Tsai C, Gerberich WW, Kruckeberg L, Kania DR (1995) Biocompatibility of Chemical-Vapour-Deposited Diamond. *Biomaterials* 16: 483-488.
- Hinuber C, Kleemann C, Friederichs RJ, Haubold L, Scheibe HJ, et al. (2010) Biocompatibility and Mechanical Properties of Diamond-Like Coatings on Cobalt-Chromium-Molybdenum Steel and Titanium-Aluminum-Vanadium Biomedical Alloys. *J Biomed Mater Res Part A* 95: 388-400.
- Achatz P, Garrido JA, Stutzmann M, Williams OA, Gruen DM, et al. (2006) Optical Properties of Nanocrystalline Diamond Thin Films. *Appl Phys Lett* 88: 101908-3.
- Williams OA (2011) Nanocrystalline Diamond. *Diam Relat Mater* 20: 621-640.
- Krueger A, Lang D (2012) Functionality Is Key: Recent Progress in the Surface Modification of Nanodiamond. *Adv Funct Mater* 22: 890-906.
- Qiang H, Makoto H, Rakesh KJ, Ashok K (2009) Structural and Electrical Characteristics of Nitrogen-Doped Nanocrystalline Diamond Films Prepared by CVD. *J Phys D* 42: 025301-025304.
- Heyer S, Janssen W, Turner S, Lu YG, Yeap WS, et al. (2014) Toward Deep Blue Nano Hope Diamonds: Heavily Boron-Doped Diamond Nanoparticles. *ACS Nano* 8: 5757-5764.
- Strobel P, Riedel M, Ristein J, Ley L (2004) Surface Transfer Doping of Diamond. *Nature* 430: 439-441.
- Hassan MM, Larsson K (2014) Effect of Surface Termination on Diamond (100) Surface Electrochemistry. *J Phys Chem C* 118: 22995-23002.
- Karlsson M, Forsberg P, Nikolajeff F (2009) From Hydrophilic to Superhydrophobic: Fabrication of Micrometer-Sized Nail-Head-Shaped Pillars in Diamond. *Langmuir* 26: 889-893.
- Grotz B, Hauf MV, Dankerl M, Naydenov B, Pezzagna S, et al. (2012) Charge State Manipulation of Qubits in Diamond. *Nat Commun* 3: 729-736.
- Hartl A, Schmiche E, Garrido JA, Hernando J, Catharino SC, et al. (2004) Protein-Modified Nanocrystalline Diamond Thin Films for Biosensor Applications. *Nat Mater* 3: 736-42.
- Man HB, Ho D (2012) Diamond as a Nanomedical Agent for Versatile Applications in Drug Delivery, Imaging, and Sensing. *Phys Stat Sol A* 209: 1609-1618.
- Stavis C. (2011) Surface Functionalization of Thin-Film Diamond for Highly Stable and Selective Biological Interfaces. *Proc Natl Acad Sci USA* 108: 983-988.
- Radadia AD, Stavis CJ, Carr R, Zeng H, King, WP, et al. (2011) Control of Nanoscale Environment to Improve Stability of Immobilized Proteins on Diamond Surfaces. *Adv Funct Mater* 21: 1040-1050.
- Xing Z. (2013) Biological Effects of Functionalizing Copolymer Scaffolds with Nanodiamond Particles. *Tissue Eng* 19: 1783-91.
- Kloss FR, et al. (2013) BMP-2 Immobilized on Nanocrystalline Diamond-Coated Titanium Screws; Demonstration of Osteoinductive Properties in Irradiated Bone. *Head & Neck* 35: 235-241.
- Hlady V, Buijs J (1996) Protein Adsorption on Solid Surfaces. *Curr Opin Biotechnol* 7: 72-77.
- Huang TS, Tzeng Y, Liu YK, Chen YC, Walker KR, et al. (2004) Immobilization of Antibodies and Bacterial Binding on Nanodiamond and Carbon Nanotubes for Biosensor Applications. *Diam Relat Mater* 13: 1098-1102.
- Paci JT, Man HB, Saha B, Ho D, Schatz GC (2013) Understanding the Surfaces of Nanodiamonds. *J Phys Chem C* 117: 17256-17267.
- Meinhardt T, Lang D, Dill H, Krueger A (2011) Pushing the Functionality of Diamond Nanoparticles to New Horizons: Orthogonally Functionalized Nanodiamond Using Click Chemistry. *Adv Funct Mater* 21: 494-500.
- Skokov S, Weiner B, Frenklach M (1997) Theoretical Study of Oxygenated (100) Diamond Surfaces in the Presence of Hydrogen. *Phys. Rev. B* 55: 1895-1902.
- Petrini D, Larsson K (2006) A Theoretical Study of the Energetic Stability and Geometry of Hydrogen- and Oxygen-Terminated Diamond (100) Surfaces. *J Phys Chem C* 111:795-801.
- Nebel CE, Shin D, Rezek B, Tokuda N, Uetsuka H, et al. (2007) Diamond and Biology. *J R Soc Interface* 4: 439-61.
- Szunerits S, Boukherroub R (2008) Different Strategies for Functionalization of Diamond Surfaces. *J Solid State Electrochem* 12: 1205-1218.
- Yang JH, Nakano Y, Murakami Y, Song KS, Kawarada H (2008) Functionalization of Ultradispersed Diamond for DNA Detection. *J Nanopart Res* 10: 69-75.
- Basiuk EV, Santamaria-Bonfil A, Meza-Laguna V, Gromovoy TY, Alvares-Zaucó E, et al. (2013) Solvent-Free Covalent Functionalization of Nanodiamond with Amines. *Appl Surf Sci* 275: 324-334.
- Holt KB (2007) Diamond at the Nanoscale: Applications of Diamond Nanoparticles from Cellular Biomarkers to Quantum Computing. *Phil Trans R Soc A* 365: 2845-2861.
- Wu Z, Cohen RE (2006) More Accurate Generalized Gradient Approximation for Solids. *Phys Rev B* 73: 235116.
- Grossman JC, Mitas L, Raghavachari K (1995) Structure and Stability of Molecular Carbon: Importance of Electron Correlation. *Phys Rev Lett* 75: 3870-3873.
- Monkhorst HJ, Pack JD (1976) Special Points for Brillouin-Zone Integrations. *Phys Rev B* 13: 5188-5192.
- Zhao S, Larsson K (2013) Theoretical Study of the Energetic Stability and

-
- Geometry of Terminated and B-Doped Diamond (111) Surfaces. *J Phys Chem C* 118: 1944-1957.
35. Krueger A (2008) Diamond Nanoparticles: Jewels for Chemistry and Physics. *Adv Mater* 20:2445-2449.
36. Pfrommer BG, Côté M, Louie SG, Cohen ML (1997) Relaxation of Crystals with the Quasi-Newton Method. *J Comput Phys* 131: 233-240.
37. Hargittai M, Hargittai I (1992) Experimental and Computed Bond Lengths: The Importance of Their Differences. *Int J Quantum Chem* 44: 1057-1067.
38. Atkins P, Overton T, Rourke J, Weller M, Armstrong F, et al. (2010) *Inorganic Chemistry*; Oxford University Press: Oxford.
39. Kuznetsov O, Sun Y, Thaner R, Bratt A, Shenoy V, et al. (2012) Water-Soluble Nanodiamond. *Langmuir* 28: 5243-8.
40. Wang X, Ruslinda AR, Ishiyama Y, Ishii Y, Kawarada H (2011) Higher Coverage of Carboxylic Acid Groups on Oxidized Single Crystal Diamond (001). *Diam Relat Mater* 20: 1319-1324.